

IMPROVED ANISOTROPIC PERMEABILITY CHARACTERIZATION IN UNIDIRECTIONAL INJECTIONS BASED ON FLOW FRONT ANGLE MEASUREMENTS

Claudio Di Fratta^{1*}, François Trochu² and Paolo Ermanni¹

¹Laboratory of Composite Materials and Adaptive Structures, ETH Zürich
Tannenstrasse 3, CH-8092 Zurich, Switzerland

*Email: claudiodifratta@mavt.ethz.ch, web page: <http://www.structures.ethz.ch>

²Center on Composites of High Performance, École Polytechnique de Montréal
P.O. Box 6079, Station "Centre-Ville", Montreal, Canada

Keywords: Experimental Characterization, Fabrics/textiles, Liquid Composite Molding (LCM), Permeability, Resin Transfer Molding (RTM)

ABSTRACT

In Liquid Composite Molding (LCM), the textile permeability characterizes the ease of establishing a resin flow through the fibrous reinforcement. This fundamental property allows simulating the preform impregnation, predicting cavity filling times and optimizing process parameters. Its knowledge gives also useful information on the quality of fabrics and finished parts.

Although the characterization of textile permeability has not been standardized yet, a recent international benchmark exercise on in-plane measurements has shown that reproducible results can be obtained by performing unidirectional (1D) injections following a recommended experimental procedure. The effective permeability along the injection direction is measured during a 1D filling test in a rectangular cavity. In order to fully characterize the in-plane permeability tensor, injections along three different directions (e.g., with fabrics oriented at 0°, 45° and 90°) must be normally conducted.

The present work shows how to reduce the number of injections required for a complete in-plane permeability characterization. In particular, new strategies are described to calculate the principal permeability values based on injections along only two directions or even only one direction of the textile. The proposed approaches rely on measurements of the flow front angle – namely, the angle between the flow front and the injection direction – along with the effective permeability. The relationship between the flow front angle and the textile permeability is illustrated and experimentally exploited for the characterization of different kinds of textiles. Results show that the anisotropic permeability of textiles can be accurately characterized with a reduced number of unidirectional injection experiments and, thus, with a considerable saving of time and material samples.

1 INTRODUCTION

Liquid Composite Molding (LCM) indicates a family of manufacturing processes for composite materials characterized by the injection or infusion of a liquid resin system into a dry fibrous preform [1]. A fundamental material property to describe the preform impregnation is the textile permeability. It represents the ability of a textile to transmit fluids. Its knowledge gives information for flow simulations, prediction of filling times, optimization of process parameters as well as indirect assessment of the quality of raw materials and finished parts [1-10].

The experimental characterization of textile permeability has not been standardized yet, although several procedures have been proposed as summarized in [11, 12]. Regarding in-plane measurements, the issued characterization procedures can be sorted into two categories by the direction of the liquid flow: radial (2D) or unidirectional (1D) flow. It has been shown that performing 1D injections allows permeability measurements with the highest reproducibility [12, 13]. Moreover, the scientific community have recently proposed common guidelines for unidirectional tests and used them in an international benchmark exercise [14], preparing the ground for a future standard.

A complete in-plane permeability characterization by 1D injections generally involves numerous tests, requiring several material samples and much time. As a matter of fact, the conventional approach to measure the principal permeability values – followed for example in the above mentioned benchmark exercise – is based on injections along three directions, where the textile is oriented at 0° , 45° and 90° with respect to, e.g., the warp (in woven fabrics) or the reference tows' direction. For each direction, the experiments should be repeated at least three times for statistical averaging and the whole series of tests should be conducted for every single fiber volume content of interest.

In our previous work [7], we have demonstrated that the number of experiments can be considerably reduced measuring concurrently the effective permeability along the test direction and the flow front angle, which is the angle between the flow front profile and the longitudinal direction of the test rig (i.e., the injection direction). In this way, injections along only two directions – or even only one, if the orientation of the principal permeability directions is known – are required for a complete in-plane characterization. In particular, the strategy developed in [7] consists of performing tests along two orthogonal directions (e.g., orienting the textile at 0° and 90°) or along one known non-principal direction (e.g., orienting the textile at 45° , while for instance the principal permeability orientation is 0°).

The present study gives an overview and makes a comparison of different strategies to characterize textile permeability through 1D injection tests. The focus is set on the novel approach based on flow front angle measurements introduced by Di Fratta et al. [7]. In the next section, we recall the concepts of effective permeability and flow front angle, illustrating their relationships with the principal permeability values and orientation. The in-plane characterization methods are presented in section 3, which collects the strategies shown in [7, 11] and introduces a new one based on tests along two directions with the textile oriented at 0° and 45° . Section 4 compares new and conventional characterization methods using the experimental results in [7], which were obtained through tests with different kinds of textiles (UD fibers, plain weave and twill fabrics). The comparison shows that the new strategies based on flow front angle measurements returned accurate permeability values in a good agreement with the results of the conventional approach. A short summary of the study is given in section 5.

2 FLOW FRONT ANGLE AND EFFECTIVE PERMEABILITY IN 1D INJECTION TESTS

Unidirectional injections for permeability measurements consist of impregnating a rectangular fibrous preform with a test liquid and recording the flow front progression over time. The guidelines for the international benchmark exercise [14] detail the recommended experimental procedure to perform the tests, setting the conditions for preform size, liquid viscosity, injection pressure, test rig set-up, etc. The flow front positions – measured during the experiments along the center line of the cavity – allow calculating the effective permeability K_γ of the preform at the tested textile orientation γ (as an example, the Least Square Fit [14] method can be employed for this purpose). Such effective permeability is related to the principal permeability values K_1 and K_2 and the principal permeability orientation ϑ by the following equation [11]:

$$K_\gamma = \frac{K_1 K_2}{K_1 \sin^2 \vartheta + K_2 \cos^2 \vartheta} = \frac{K_1 \beta}{\sin^2 \vartheta + \beta \cos^2 \vartheta} \quad (1)$$

where β is the degree of anisotropy, defined as:

$$\beta = \frac{K_2}{K_1} \quad (2)$$

and takes value between 0 and 1 ($0 < \beta \leq 1$). Note that the three parameters K_1 , K_2 and ϑ (or equivalently K_1 , β and ϑ) completely define the in-plane permeability of a textile and can be used to calculate the permeability tensor [11].

In the case of anisotropic permeability ($\beta \neq 1$), Di Fratta et al. [7] show that the flow front profile may not be perpendicular to the test direction. The angle that the flow front forms with the longitudinal direction of the test rig – indicated in Fig. 1 with the symbol α_γ – depends on the degree of

anisotropy β and the principal permeability orientation ϑ . The formula of such flow front angle (relative to the tested textile orientation γ) is [7]:

$$\alpha_\gamma = \tan^{-1} \left(\frac{\sin^2 \vartheta + \beta \cos^2 \vartheta}{(1 - \beta) \sin \vartheta \cos \vartheta} \right) \quad (3)$$

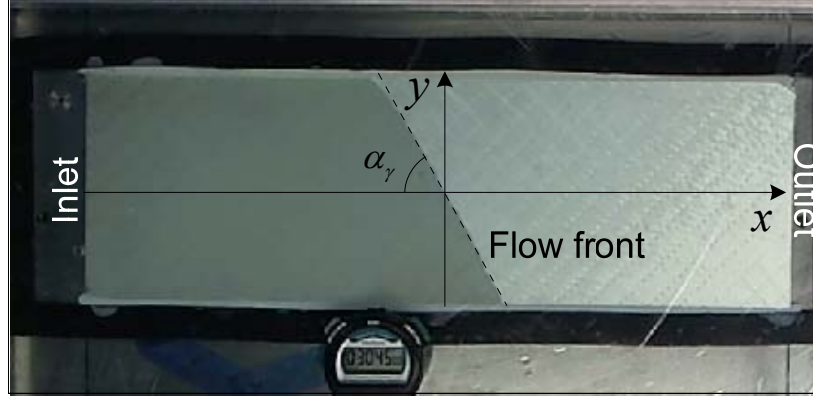


Figure 1: Flow front angle in a unidirectional injection test with UD fibers oriented at $\gamma = 45^\circ$.

From equation (3), it is possible to obtain $\alpha_\gamma = 90^\circ$ when the permeability is isotropic ($\beta = 1$) or the textile is impregnated along a principal permeability direction ($\vartheta = 0^\circ$ or $\vartheta = 90^\circ$). It is worth noticing that, in order to have a minimum influence of the preform boundaries, the flow front angle as well as the effective permeability should be measured in the central zone of the textile when the flow front is sufficiently far from the inlet line. In addition, we point out that, as an alternative to visual flow front observations, both K_γ and α_γ can be measured by only three pressure sensors opportunely located in the mold [7]. Note finally that the relationship between flow front angle and textile permeability is graphically represented in Fig. 2, where the flow front angle α_γ represents the slope of the tangent to the permeability ellipse at the intersection to the test direction (x-axis), as also demonstrated in [7].

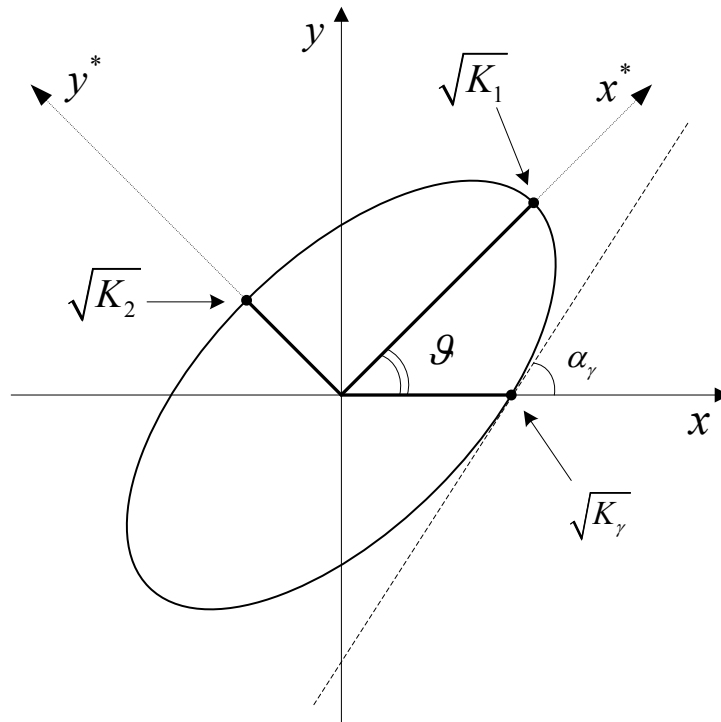


Figure 2: Permeability ellipse and flow front angle.

3 IN-PLANE PERMEABILITY CHARACTERIZATION STRATEGIES

Measurements of the effective permeability and the flow front angle allow assessing the in-plane permeability through the two independent equations (1) and (3). Since three parameters (K_1 , K_2 and ϑ) have to be evaluated for a complete in-plane characterization, injection tests along at least two different textile directions must be conducted, in order to get a system with enough equations for the number of unknowns. The textile directions to test can be, however, reduced to only one if the principal permeability orientation ϑ is known before the experiments (for example, it may be estimated from geometrical characteristics of the textile). In this section, we illustrate four characterization strategies based on different combinations of textile orientations in the injection tests. In particular, the textile orientations 0° , 45° and 90° (with respect to the warp or to UD fibers' direction) are considered.

3.1 Strategy A: Injection tests with textile oriented at 0° , 45° and 90°

The first strategy represents the conventional characterization method, which is used in the international benchmark exercise [14]. Measurements of the flow front angle are not taken into consideration and the in-plane permeability is characterized employing only the effective permeability values K_{0° , K_{45° and K_{90° measured in tests with textile oriented at 0° , 45° and 90° , respectively. Using the expression of the effective permeability (1), it is possible to calculate the principal permeability orientation ϑ and, hence, the values K_1 and K_2 through the following equations, derived from [11]:

$$\vartheta = \frac{1}{2} \tan^{-1} \left(\frac{K_{0^\circ}K_{45^\circ} + K_{45^\circ}K_{90^\circ} - 2K_{0^\circ}K_{90^\circ}}{K_{0^\circ}K_{45^\circ} - K_{45^\circ}K_{90^\circ}} \right) \quad (4)$$

$$K_1 = \frac{2K_{0^\circ}K_{90^\circ} \cos 2\vartheta}{K_{0^\circ}(\cos 2\vartheta - 1) + K_{90^\circ}(\cos 2\vartheta + 1)} \quad (5)$$

$$K_2 = \frac{2K_{0^\circ}K_{90^\circ} \cos 2\vartheta}{K_{0^\circ}(\cos 2\vartheta + 1) + K_{90^\circ}(\cos 2\vartheta - 1)} \quad (6)$$

The degree of anisotropy is then given introducing equations (5) and (6) in (2):

$$\beta = \frac{K_2}{K_1} = \frac{K_{0^\circ}(\cos 2\vartheta - 1) + K_{90^\circ}(\cos 2\vartheta + 1)}{K_{0^\circ}(\cos 2\vartheta + 1) + K_{90^\circ}(\cos 2\vartheta - 1)} \quad (7)$$

3.2 Strategy B: Injection tests with textile oriented at 0° and 90°

This second strategy is derived from our previous work [7], where we show that, when the flow front angle and the effective permeability are measured along two orthogonal textile directions, an analytical solution of the resulting system of equations (1) and (3) for both directions can be obtained. In particular, choosing the textile orientations 0° and 90° , it follows from the respective measured angles α_{0° and α_{90° :

$$\vartheta = \frac{1}{2} \tan^{-1} \left(-\frac{2}{\tan \alpha_{0^\circ} - \tan \alpha_{90^\circ}} \right) \quad (8)$$

$$\beta = \frac{(\tan \alpha_{0^\circ} - \tan \alpha_{90^\circ}) \sin 2\vartheta - 2}{(\tan \alpha_{0^\circ} - \tan \alpha_{90^\circ}) \sin 2\vartheta - 2} \quad (9)$$

and, from there, the principal permeability values are calculated using also K_{0° (the measurement of K_{90° is here redundant):

$$K_1 = K_{0^\circ}(\sin^2 \vartheta + \beta \cos^2 \vartheta) / \beta \quad (10)$$

$$K_2 = K_1 \beta = K_{0^\circ}(\sin^2 \vartheta + \beta \cos^2 \vartheta) \quad (11)$$

It is worth highlighting that, if it results $\alpha_{0^\circ} = 90^\circ$, then the orientation 0° corresponds to a principal permeability direction (and the orientation 90° to the other one). In such a case, the highest between K_{0° and K_{90° will represent K_1 and define the value of ϑ (either equal to 0° or 90°), while the lowest will

represent K_2 . If $\alpha_{0^\circ} = 90^\circ$ and $K_{0^\circ} = K_{90^\circ}$, the permeability is isotropic.

3.3 Strategy C: Injection tests with textile oriented at 0° and 45°

The third strategy is similar to the second one, but the textile orientation 45° replaces the orientation 90° . Using the equations developed in the appendix, the in-plane permeability may be assessed from K_{0° , K_{45° and α_{0° . For this purpose, the degree of anisotropy β is initially calculated by solving the following implicit equation:

$$\frac{K_{0^\circ} \tan \alpha_{45^\circ}}{K_{0^\circ} + K_{45^\circ} \tan \alpha_{45^\circ}} \frac{1 + \beta}{2} - \sin^2 \left(\frac{1}{2} \sin^{-1} \left(\frac{K_{0^\circ}}{K_{0^\circ} + K_{45^\circ} \tan \alpha_{45^\circ}} \frac{1 + \beta}{1 - \beta} \right) \right) - \beta \cos^2 \left(\frac{1}{2} \sin^{-1} \left(\frac{K_{0^\circ}}{K_{0^\circ} + K_{45^\circ} \tan \alpha_{45^\circ}} \frac{1 + \beta}{1 - \beta} \right) \right) = 0 \quad (12)$$

and, then, the parameters K_1 , K_2 and ϑ are evaluated as follows:

$$K_1 = \frac{K_{0^\circ} K_{45^\circ} \tan \alpha_{45^\circ}}{K_{0^\circ} + K_{45^\circ} \tan \alpha_{45^\circ}} \frac{1 + \beta}{2\beta} \quad (13)$$

$$K_2 = K_1 \beta = \frac{K_{0^\circ} K_{45^\circ} \tan \alpha_{45^\circ}}{K_{0^\circ} + K_{45^\circ} \tan \alpha_{45^\circ}} \frac{1 + \beta}{2} \quad (14)$$

$$\vartheta = \frac{1}{2} \cos^{-1} \left(\frac{K_{0^\circ}}{K_{0^\circ} + K_{45^\circ} \tan \alpha_{45^\circ}} \frac{1 + \beta}{1 - \beta} \right) \quad (15)$$

Numerical techniques such as constrained optimizations could be employed to solve equation (12). Nevertheless, the solution may be not accurate since this approach is subjected to limitations as mentioned in the appendix.

3.4 Strategy D: Injection tests with textile oriented at 45°

In this last strategy, the principal permeability orientation is supposed known. As above mentioned, it may be assessed from the textile architecture; for instance, it is reasonable to assume that the direction of K_1 in a UD fiber tape corresponds to the tows' direction. In this case, our previous work [7] shows that the principal permeability values can be simply calculated from the flow front angle and the effective permeability measured along only one non-principal textile direction. If the principal permeability orientation is 0° , the measurement of the flow front angle α_{45° with the textile oriented at 45° allows the direct evaluation of β rearranging equation (3):

$$\beta = \frac{\tan \alpha_{45^\circ} - 1}{\tan \alpha_{45^\circ} + 1} \quad (16)$$

Using then the measurement of K_{45° and equations (1) and (2), we obtain finally:

$$K_1 = \frac{K_{45^\circ}(1 + \beta)}{2\beta} \quad (17)$$

$$K_2 = K_1 \beta = \frac{K_{45^\circ}(1 + \beta)}{2} \quad (18)$$

4 EXPERIMENTAL RESULTS AND DISCUSSION

The comparison among the above illustrated characterization strategies is based on the experiments performed by Di Fratta et al. [7]. The tests involved three textiles with different architectures as listed in Table 1. For all three textiles, the principal permeability orientations were close to 0° ($|\vartheta| < 5^\circ$). This confirmed that the strategy D was applicable, since the textile orientations 0° and 90° corresponded approximately to the directions of K_1 and K_2 , respectively.

As far as the uncertainty analysis is concerned, the standard deviations of the permeability results were calculated from the statistical errors of the flow front angle and effective permeability

measurements. In particular, the measurements were considered independent and the following law of error propagation was applied:

$$\sigma_f = \sqrt{\sum_{\gamma} \left(\left(\frac{\partial f}{\partial K_{\gamma}} \sigma_{K_{\gamma}} \right)^2 + \left(\frac{\partial f}{\partial \alpha_{\gamma}} \sigma_{\alpha_{\gamma}} \right)^2 \right)} \quad (19)$$

where σ_f is the standard deviation of the generic parameter f (i.e., K_1 , K_2 , β or ϑ), while $\sigma_{K_{\gamma}}$ and $\sigma_{\alpha_{\gamma}}$ are the standard deviations of the effective permeability and flow front angle, respectively, obtained from the tests with textile oriented at γ (equal to 0° , 45° or 90°). The derivatives of f in (19) were computed from the corresponding equations in section 3. For the strategy C, the standard deviation of β was roughly assessed with $\sigma_{\beta} = 0.03$ for all the textiles.

Textile architecture	Material	V_f (%)	Supplier	ID Number
UD fiber tape	Glass	42.0 ± 0.3	Tissa Glasweberei AG	850.0445.80.0600
Plain weave	Glass	42.9 ± 0.8	Tissa Glasweberei AG	850.0470.01.1240
2/2 Twill weave	Glass	42.1 ± 0.4	Suter Kunststoffe AG	190.1458

Table 1: Textiles used in the tests at the indicated fiber volume content V_f [7].

The following figures and tables display the results of the permeability characterization using the different strategies for the UD fibers, plain weave and twill weave fabrics.

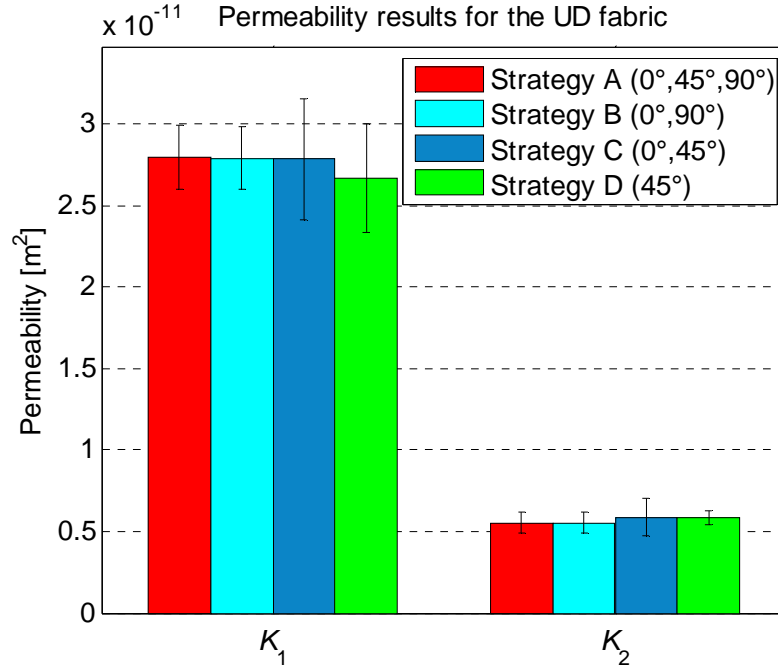


Figure 3: Comparison of principal permeability values for the UD fabric.

UD fibers	K_1 [10^{-11} m^2]	K_2 [10^{-11} m^2]	β [-]
Strategy A	2.797 ± 0.195 ($\pm 7.0\%$)	0.554 ± 0.063 ($\pm 11.4\%$)	0.198 ± 0.029
Strategy B	2.790 ± 0.193 ($\pm 6.9\%$)	0.554 ± 0.062 ($\pm 11.2\%$)	0.199 ± 0.026
Strategy C	2.786 ± 0.373 ($\pm 13.4\%$)	0.588 ± 0.115 ($\pm 19.5\%$)	0.211 ± 0.030
Strategy D	2.670 ± 0.335 ($\pm 12.5\%$)	0.582 ± 0.043 ($\pm 7.4\%$)	0.218 ± 0.027

Table 2: Permeability characterization results for the UD fabric.

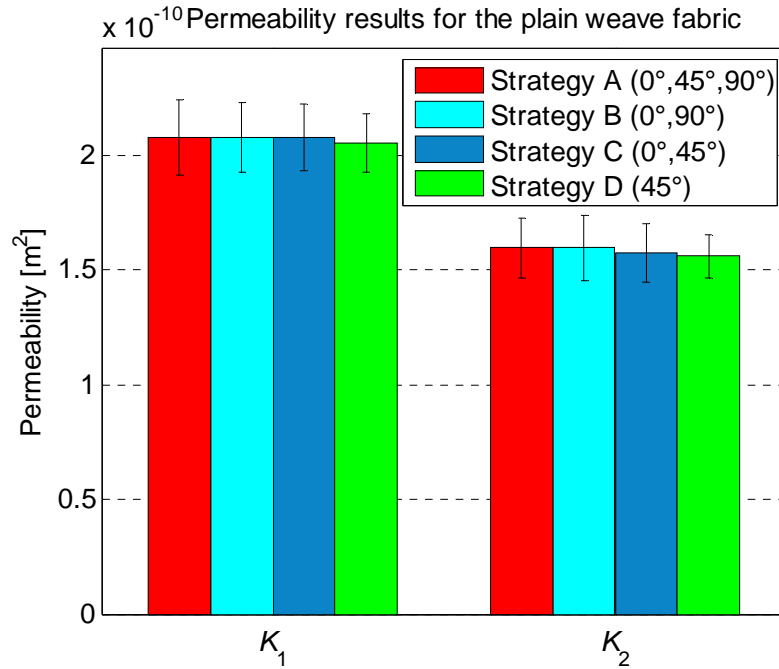


Figure 4: Comparison of principal permeability values for the plain weave fabric.

Plain weave	K_1 [10^{-11} m^2]	K_2 [10^{-11} m^2]	β [-]
Strategy A	20.784 ± 1.641 (± 7.9 %)	15.941 ± 1.332 (± 8.4 %)	0.767 ± 0.086
Strategy B	20.753 ± 1.516 (± 7.3 %)	15.959 ± 1.435 (± 9.0 %)	0.769 ± 0.089
Strategy C	20.754 ± 1.447 (± 7.0 %)	15.711 ± 1.260 (± 8.0 %)	0.757 ± 0.030
Strategy D	20.530 ± 1.274 (± 6.2 %)	15.583 ± 0.944 (± 6.1 %)	0.759 ± 0.028

Table 3: Permeability characterization results for the plain weave fabric.

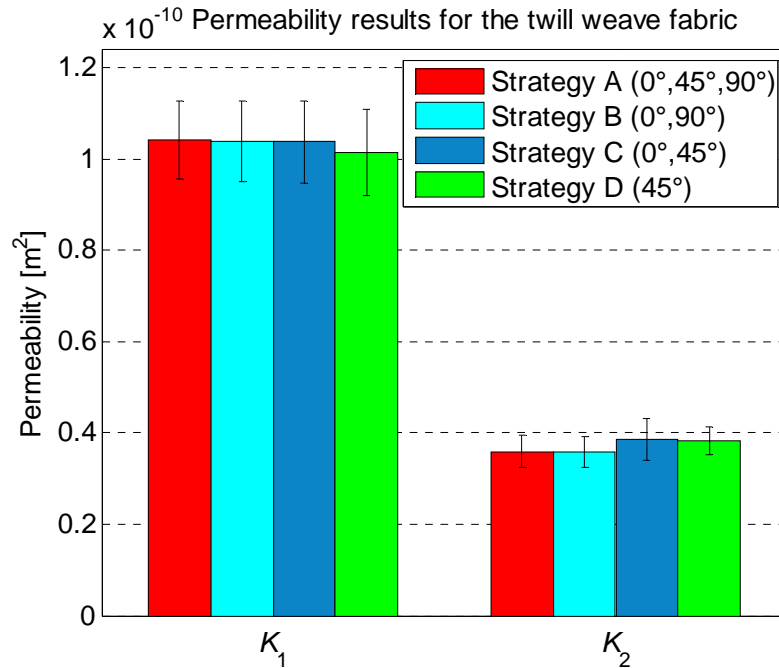


Figure 5: Comparison of principal permeability values for the twill weave fabric.

Twill weave	$K_1 [10^{-11} \text{ m}^2]$	$K_2 [10^{-11} \text{ m}^2]$	$\beta [-]$
Strategy A	$10.420 \pm 0.862 (\pm 8.3 \%)$	$3.595 \pm 0.345 (\pm 9.6 \%)$	0.345 ± 0.046
Strategy B	$10.389 \pm 0.877 (\pm 8.4 \%)$	$3.599 \pm 0.333 (\pm 9.3 \%)$	0.346 ± 0.043
Strategy C	$10.391 \pm 0.905 (\pm 8.7 \%)$	$3.866 \pm 0.459 (\pm 11.9 \%)$	0.372 ± 0.030
Strategy D	$10.137 \pm 0.947 (\pm 9.3 \%)$	$3.830 \pm 0.318 (\pm 8.3 \%)$	0.378 ± 0.024

Table 4: Permeability characterization results for the twill weave fabric.

The above figures and tables show that the principal permeability values were accurately determined for all three textiles. The different strategies returned virtually equivalent results, confirming that the new methods based on flow front angle measurements allow characterizing the in-plane permeability consistently with the reference method (strategy A) as well as more efficiently, since fewer experiments were required.

Final comments on each strategy, considering also practical issues, are below given:

- Strategy A is the conventional approach and requires the highest number of tests and material samples.
- Strategy B allows reducing the number of tests by one third compared to strategy A, without needing experiments with the textile oriented at 45° . This brings the additional advantage that the material samples are easily cut out of the fabric roll with less scrap. However, it may be difficult to finely assess the principal permeability orientation if it is very close to 0° or 90° (one of the test direction), because the flow front angle would visibly appear equal to 90° .
- Strategy C is based on the same number of tests as strategy B, but the duration of the injections is shorter if $\vartheta \approx 0^\circ$. In such a case, the orientation 90° represents approximately the direction of K_2 , which is the less favorable to the flow. As an example, regarding the experiments with the UD fabric performed in this work, each injection at 90° lasted about 3 hours, while the ones at 45° took a little more than 1.5 hours using the same injection pressure. On the other hand, the calculation of the principal permeability values through this characterization strategy involve the numerical solution of equation (12), which is generally troublesome and may generate errors (see also the appendix).
- Strategy D is the most efficient because it requires the lowest number of tests, but the principal permeability orientation (around 0°) has to be estimated in advance.

5 CONCLUSIONS

This work shows how to characterize the in-plane permeability through 1D injection tests in an accurate and efficient way, by using concurrent flow front angle and effective permeability measurements. Based on such measurements, different characterization strategies were developed and experimentally investigated. The new strategies returned results comparable to the conventional approach, but they required a reduced number of injection tests. This allowed complete in-plane permeability characterizations with fewer material samples, in less time and, thus, at lower costs.

ACKNOWLEDGEMENTS

The authors acknowledge Dr. Florian Klunker and Grigorios Koutsoukis for their collaboration to the work.

APPENDIX

The present appendix derives the equations for in-plane permeability characterization through 1D injection tests along two directions forming an angle of 45° . As an example, the first textile orientation is γ and the second one is $\delta = \gamma + 45^\circ$. Naming ϑ and φ respectively the principal permeability orientations with the textile oriented at γ and δ , it follows that $\varphi = \vartheta + 45^\circ$. Considering equations (1) and (3), we write the following quantities measured during the tests:

$$K_\gamma = \frac{K_1\beta}{\sin^2\vartheta + \beta\cos^2\vartheta} \quad K_\delta = \frac{K_1\beta}{\sin^2\varphi + \beta\cos^2\varphi} \quad \tan\alpha_\delta = \frac{\sin^2\varphi + \beta\cos^2\varphi}{(1-\beta)\sin\varphi\cos\varphi} \quad (20)$$

Using the trigonometric relationships:

$$\sin\vartheta = \sin(\varphi - 45^\circ) = \sin\varphi\cos45^\circ - \cos\varphi\sin45^\circ = (\sin\varphi - \cos\varphi)\sqrt{2}/2 \quad (21)$$

$$\cos\vartheta = \cos(\varphi - 45^\circ) = \cos\varphi\cos45^\circ + \sin\varphi\sin45^\circ = (\sin\varphi + \cos\varphi)\sqrt{2}/2 \quad (22)$$

the effective permeability with the textile oriented at γ becomes:

$$K_\gamma = \frac{2K_1\beta}{(\sin\varphi - \cos\varphi)^2 + \beta(\sin\varphi + \cos\varphi)^2} = \frac{2K_1\beta}{1 + \beta - 2(1-\beta)\sin\varphi\cos\varphi} \quad (23)$$

From K_δ and $\tan\alpha_\delta$ in equation (20), it results:

$$\sin^2\varphi + \beta\cos^2\varphi = \frac{K_1\beta}{K_\delta} = (1-\beta)\sin\varphi\cos\varphi\tan\alpha_\delta \Rightarrow (1-\beta)\sin\varphi\cos\varphi = \frac{K_1\beta}{K_\delta\tan\alpha_\delta} \quad (24)$$

which, replaced in equation (23), leads to:

$$K_\gamma = \frac{2K_1\beta K_\delta \tan\alpha_\delta}{(1+\beta)K_\delta \tan\alpha_\delta - 2K_1\beta} \Rightarrow 2K_1\beta(K_\gamma + K_\delta \tan\alpha_\delta) - (1+\beta)K_\gamma K_\delta \tan\alpha_\delta = 0 \quad (25)$$

Once β is found, equation (25) allows calculating K_1 and K_2 as follows:

$$K_1 = \frac{K_\gamma K_\delta \tan\alpha_\delta}{K_\gamma + K_\delta \tan\alpha_\delta} \frac{1+\beta}{2\beta} \quad K_2 = K_1\beta = \frac{K_\gamma K_\delta \tan\alpha_\delta}{K_\gamma + K_\delta \tan\alpha_\delta} \frac{1+\beta}{2} \quad (26)$$

From equations (24) and (26), we get:

$$\sin 2\varphi = 2\sin\varphi\cos\varphi = \frac{2K_1\beta}{(1-\beta)K_\delta \tan\alpha_\delta} = \frac{K_\gamma}{K_\gamma + K_\delta \tan\alpha_\delta} \frac{1+\beta}{1-\beta} \quad (27)$$

and, hence, it is possible to express φ or, equivalently, ϑ as a function of the sole unknown β :

$$\varphi = \frac{1}{2}\sin^{-1}\left(\frac{K_\gamma}{K_\gamma + K_\delta \tan\alpha_\delta} \frac{1+\beta}{1-\beta}\right) \quad \vartheta = \frac{1}{2}\cos^{-1}\left(\frac{K_\gamma}{K_\gamma + K_\delta \tan\alpha_\delta} \frac{1+\beta}{1-\beta}\right) \quad (28)$$

where the last equation is obtained noting that $\sin 2\varphi = \sin 2(\vartheta + 45^\circ) = \cos 2\vartheta$. It is worth pointing out that, in order to get real solutions from (28), the degree of anisotropy β must fulfill the following condition:

$$\beta \leq \frac{K_\delta \tan\alpha_\delta}{2K_\gamma + K_\delta \tan\alpha_\delta} \quad (29)$$

Finally, using equations (26) and (28), the expression of K_δ in (20) can be rearranged so as to obtain an equation for finding the degree of anisotropy β :

$$K_1\beta - K_\delta\sin^2\vartheta - K_\delta\beta\cos^2\vartheta \Rightarrow \frac{K_\gamma \tan\alpha_\delta}{K_\gamma + K_\delta \tan\alpha_\delta} \frac{1+\beta}{2} - \sin^2\left(\frac{1}{2}\sin^{-1}\left(\frac{K_\gamma}{K_\gamma + K_\delta \tan\alpha_\delta} \frac{1+\beta}{1-\beta}\right)\right) - \beta\cos^2\left(\frac{1}{2}\sin^{-1}\left(\frac{K_\gamma}{K_\gamma + K_\delta \tan\alpha_\delta} \frac{1+\beta}{1-\beta}\right)\right) = 0 \quad (30)$$

Consequently, the equations (12), (13), (14) and (15) for the characterization strategy C result from equations (26), (28) and (29) in the case that $\gamma = 0^\circ$ and $\delta = 45^\circ$. In this work, the solution of (30) was found seeking the value of β that minimizes the left-hand member of the equation within the constraint (29). Nevertheless, this approach – and the overall solution procedure presented in this appendix – may be not applicable in all cases and could lead to errors depending on the relative orientation of the principal permeability directions with respect to the test directions.

REFERENCES

- [1] P. Ermanni, C. Di Fratta and F. Trochu, *Molding: Liquid Composite Molding (LCM)*, In: Wiley Encyclopedia of Composites, 2nd Edition, Wiley, 2012, pp 1884-1893.
- [2] R. Gauvin, F. Trochu, Y. Lemenn and L. Diallo, Permeability measurement and flow simulation through fiber reinforcement, *Polymer Composites*, **17**, 1996, pp. 34-42 (doi: [10.1002/pc.10588](https://doi.org/10.1002/pc.10588)).
- [3] F. Trochu, E. Ruiz, V. Achim and S. Soukane, Advanced numerical simulation of liquid composite molding for process analysis and optimization, *Composites Part A: Applied Science and Manufacturing*, **37**, 2006, pp. 890–902 (doi: [10.1016/j.compositesa.2005.06.003](https://doi.org/10.1016/j.compositesa.2005.06.003)).
- [4] C. Di Fratta, F. Klunker and P. Ermanni, A methodology for flow-front estimation in LCM processes based on pressure sensors, *Composites Part A: Applied Science and Manufacturing*, **47**, 2013, pp. 1–11 (doi: [10.1016/j.compositesa.2012.11.008](https://doi.org/10.1016/j.compositesa.2012.11.008)).
- [5] C. Di Fratta, L. Di Lillo, F. Klunker and P. Ermanni, Detection of permeability variations for early quality assessment in liquid composite molding, *Proceedings of 19th International Conference on Composite Materials (ICCM 19), Montreal, Canada, July 28-August 2, 2013*, Canadian Association for Composite Structures and Materials, 2013, pp. 5439-5447.
- [6] B.M. Louis, C. Di Fratta, M. Danzi, M. Zogg and P. Ermanni, Improving time effective and robust techniques for measuring in-plane permeability of fibre preforms for LCM processing, *Proceedings of SAMPE Europe 32nd International Technical Conference & Forum (SEICO 11), Paris, France, March 28-29, 2011*, SAMPE Europe Conferences, Riehn, 2011, pp. 204-211.
- [7] C. Di Fratta, G. Koutsoukis, F. Klunker, F. Trochu and P. Ermanni, Characterization of anisotropic permeability from flow front angle measurements, *Polymer Composites*, 2015 (doi: [10.1002/pc.23382](https://doi.org/10.1002/pc.23382)).
- [8] C. Di Fratta, F. Klunker and P. Ermanni, RTM process monitoring by pressure sensors, *JEC Composites Magazine*, **91**, 2014, pp. 50–51.
- [9] C. Demaria, E. Ruiz and F. Trochu, In-plane anisotropic permeability characterization of deformed woven fabrics by unidirectional injection. Part I: Experimental results, *Polymer Composites*, **28**, 2007, pp. 797–811 (doi: [10.1002/pc.20107](https://doi.org/10.1002/pc.20107)).
- [10] C. Di Fratta, F. Klunker and P. Ermanni, Efficient method to characterize textile permeability as a function of fiber volume content with a single unidirectional injection experiment, *Proceedings of 12th International Conference on Flow Processing in Composite Materials (FPCM 12), Enschede, Netherlands, July 14-16, 2014*, University of Twente, Engineering Technology faculty, Enschede, 2014.
- [11] J.R. Weitzenböck, R.A. Shenoi and P.A. Wilson, Measurement of principal permeability with the channel flow experiment, *Polymer Composites*, **20**, 1999, pp. 321–335 (doi: [10.1002/pc.10359](https://doi.org/10.1002/pc.10359)).
- [12] S. Sharma and D.A. Siginer, Permeability measurement methods in porous media of fiber reinforced composites, *Applied Mechanics Reviews*, **63**, 2010 (doi: [10.1115/1.4001047](https://doi.org/10.1115/1.4001047)).
- [13] T.S. Mesogitis, A.A. Skordos and A.C. Long, Uncertainty in the manufacturing of fibrous thermosetting composites: A review, *Composites Part A: Applied Science and Manufacturing*, **57**, 2014, pp. 1–11 (doi: [10.1016/j.compositesa.2013.11.004](https://doi.org/10.1016/j.compositesa.2013.11.004)).
- [14] N. Vernet, E. Ruiz, S. Advani, J.B. Alms, M. Aubert, M. Barburski, B. Barari, J.M. Beraud, D.C. Berg, N. Correia, M. Danzi, T. Delavière, M. Dickert, C. Di Fratta, P. Ermanni, G. Francucci, J.A. Garcia, A. George, C. Hahn, F. Klunker, S.V. Lomov, A. Long, B. Louis, J. Maldonado, R. Meier, V. Michaud, H. Perrin, K. Pillai, E. Rodriguez, F. Trochu, S. Verheyden, M. Weitgreffe, W. Xiong, S. Zaremba and G. Ziegmann, Experimental determination of the permeability of engineering textiles: Benchmark II, *Composites Part A: Applied Science and Manufacturing*, **61**, 2014, pp. 172–184 (doi: [10.1016/j.compositesa.2014.02.010](https://doi.org/10.1016/j.compositesa.2014.02.010)).